A Steel Moment–Resisting Frame Retrofitted with Hysteretic and Viscous Devices

Gustavo L. Palazzo, Francisco A. Calderón, Víctor A. Roldán, Francisco López–Almansa

Abstract— **Energy dissipators are a convenient option for earthquake–resistant retrofitting of buildings; when a construction incorporating these systems is shaken by a strong ground motion, the devices absorb most of the damaging part of the input energy, thus protecting the main structure. Although energy dissipators have repeatedly proven their capacity to reduce the seismic response, one of the most controversial issues is their seismic efficiency under near–fault inputs. For this reason, this paper presents a numerical study about the seismic performance under near–source excitations of a structure retrofitted with hysteretic and with viscous devices. The considered structure is a symmetric 4–story steel moment–resisting unbraced frame. This structure was tested at the E–defense laboratory (Japan) under a near–fault ground motion recorded in Takatori during the Kobe earthquake (16/01/1995); this input caused the collapse of the frame. In the paper the main characteristics of the frames are presented, the design of the energy dissipators is described, and the response of the frame with/without dissipators is shown. Finally, the possibilities of improving the behavior of a building with different kind of passive energy dissipating systems are analyzed in the conclusions.**

I. Introduction

Energy dissipators are intended to consume a big portion of the input seismic energy. This energy dissipation decreases the demand on the structural systems, thereby reducing its dynamic response during an earthquake [1–3]. Thus, supplemental damping systems are usually distributed throughout a construction to absorb the energy transmitted from the ground into the primary structure [1].

Passive energy dissipating systems can be broadly classified into three different categories:

- Displacement–activated devices, like metallic dampers, friction dampers and self–centering dampers. These devices dissipate energy through the relative displacement that occur between their connecting points.
- Velocity–activated devices, like viscous dampers. These devices dissipate energy through the relative velocities that occur between their connecting points.
- Motion–activated devices, like the tuned mass dampers. These devices disturb the flow of energy in the structure through the vibration of a secondary system [1].

In this paper, two types of passive energy dissipating systems are considered: a displacement–activated device, and a velocity–activated device. The first device is a buckling restrained brace (BRB) and the second device is a viscous damper.

- Buckling-restrained braces are one of the dissipators that have been mostly used, mainly for seismic protection of building frames [4–7]. They consist of slender steel bars connected usually to the frame to be protected either like concentric diagonal braces or like concentric chevron braces. Under horizontal seismic excitations, the inter-story drift motion generates tensile and compressive axial strains in such steel bars beyond their yielding points. The buckling of these core bars is prevented by embedding them in a stockiest encasing; such casing is usually composed either of steel elements or of mortar coated with steel. Some sliding interface between the steel core and the surrounding material is required to prevent excessive shear stress transfer, since it would reduce the longitudinal stress in the core thus impairing the energy dissipation capacity.
- Typically, a fluid damper incorporates a stainless steel piston with a bronze orifice head. The device is filled with oil. The piston head utilizes specially-shaped orifices that alter the flow characteristics with the fluid relative velocity. The force produced by the damper is generated by the differential of pressure across the piston head [4, 8].

The aim of this work is to study the behavior of a particular building retrofitted with buckling–restrained braces (BRBs) and with viscous dampers devices, when the construction is subjected to a recorded near–fault motion. A comparison of the response of the building, with/without these two types of energy dissipators, in terms of displacement and acceleration, is performed.

A building is a symmetric 4–story steel moment–resisting frame, that was dynamically tested to collapse in 2007 at the shaking table of the E–Defense laboratory [9–11]. The experiments consisted in applying to the frame a 3–D scaled version of a near–fault motion recorded during the Kobe earthquake (16/01/1995). Geometry, mechanical parameters and other characteristics of the building are presented in section II. Also in that section, the numerical simulation of the building is shown. To study the accuracy of this model, numerical and experimental results are compared.

G. L. Palazzo, F. A. Calderón and V. E. Roldan, National Technological University, Ceredetec, Mendoza (e–mail: gpalazzo@frm.utn.edu.ar, francisco.calderon@frm.utn.edu.ar and victor_roldan890@hotmail.com).

F. López–Almansa, Technical University of Catalonia, Architecture Structures Department, Barcelona, Spain (e–mail: francesc.lopez–almansa@upc.edu).

The design procedures for the metallic and viscous dampers are described in section III. As well, it is explained how the dissipators were modelled.

The numerical behavior of the structure with/without dissipators is shown in section IV. Maximum displacements and accelerations in each floor are presented, as well as time histories of the top floor relative displacements and absolute accelerations.

In the conclusion, the possibility of retrofitting a building subject to near–fault inputs with energy dissipators is highlighted.

II. CONSIDERED STRUCTURE

The tested prototype is described in the first part of this section, and then, its numerical model is presented.

A. Description of the structure

The prototype, which is presented in Figure 1, is a full–scale 3D steel frame. The 3D structure has four–story steel moment resisting frames. This construction was tested under dynamic conditions to collapse in September 2007 on the world's largest three–dimensional shaking table located at Miki City, Hyogo Prefecture, Japan. The building had external walls, which consisted in autoclaved, aerated concrete panels, 0.125 m thick, fixed on to the support beams at the top and the bottom of their edges. In addition, there were internal partitions, which were made using light gauge steel backing board installed on aluminum frames.

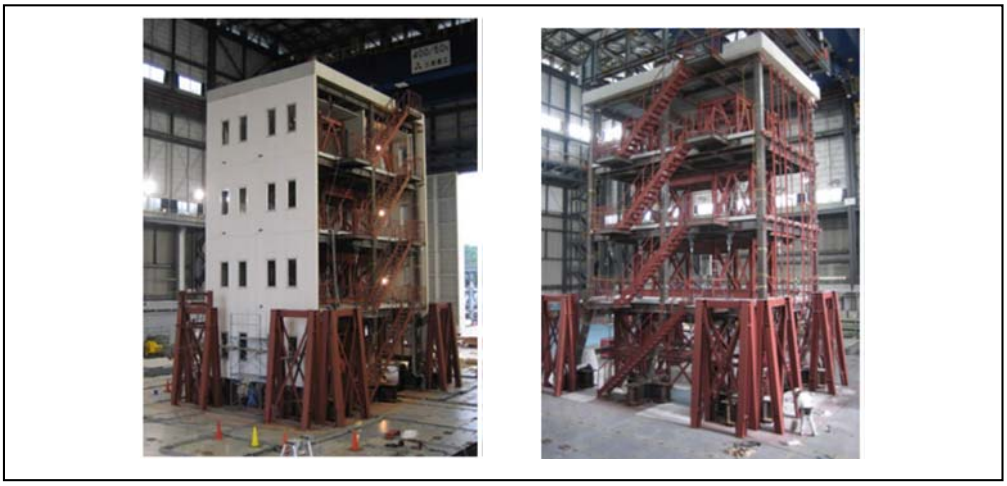

Figure 1. Specimen tested in the E–Defense Laboratory (Japan)

The frames consisted in square tube columns and composite beams with wide flanges girders. At each floor, there were also secondary beams. Slabs at second, third and fourth levels consisted in a composite deck floor with 175 mm height. The roof floor was a reinforced concrete slab, with a flat steel deck at its bottom, with an overall thickness of 150 mm. The first floor columns were rigidly connected to 1.5 m high supporting concrete blocks; in their turn, the blocks were clamped to the shaking table.

In the longitudinal direction the length of each bay was 5.0 m, while in the transversal direction the length of the bay was 6.0 m. Inter–story height was 3.875 m in the first story, and 3.5 m in the other stories.

The prototype's geometry is shown in Figure 2, and the geometry of the main beams and columns are presented in Table I.

TABLE I. MAIN BEAMS AND COLUMNS GEOMETRY

Beams				**Columns**	
Floor	**G1**	**G11**	**G12**	**Story**	**–**
5	H – 346×174×6×9	H – 346×174×6×9	H – 346×174×6×9	4	RHS – 300×300×9
4	H – 350×175×7×11	H – 350×175×7×11	H – 340×175×9×14	3	RHS – 300×300×9
3	H – 396×199×7×11	H – 400×200×8×13	H – 400×200×8×113	2	RHS – 300×300×9
2	H – 400×200×8×13	H – 400×200×8×13	H – 390×200×10×16	1	RHS – 300×300×9

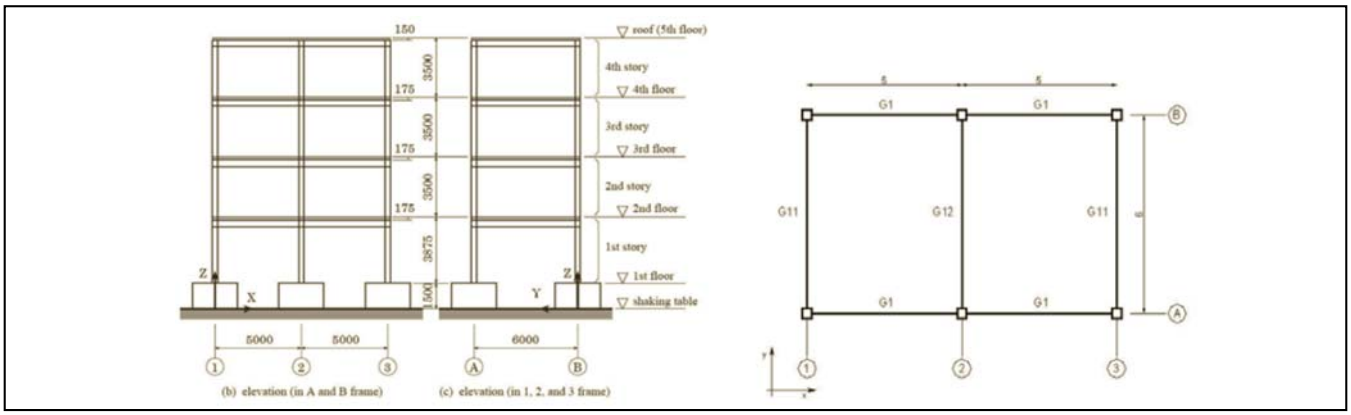

Figure 2. Prototype's geometry

The beam–column connections were detailed according to the practice developed following the 1995 Hyogoken–Nanbu earthquake (01/16/1995) to force the formation of plastic hinges out of the joints. A typical beam–column connection is displayed in Figure 3.

Figure 3. Beam–column conection

The weights of the each story of the prototype are given in Table II.

TABLE II. PROTOTYPE'S WEIGHT [KN]

Floor	Weight [kN]
5	631.5
4	476.5
3	473.0
2	474.5
Total	2055.5

The building underwent three scaled versions of the near–fault motion recorded in Takatori during the 1995 Kobe earthquake. The considered scale factors were: 40%, 60% and 100%. The peak ground accelerations for each version of the input are shown in Table III.

TABLE III. PEAK GROUND ACCELERATIONS (PGA [M/S^2]) FOR THE SCALED VERSION OF THE TAKATORI RECORD

Component	Scale factor		
	40%	60%	100%
North–South	3.028	4.658	8.566
East–West	3.327	5.451	8.492
Vertical	1.429	2.348	3.848

The North–South component was applied in the longitudinal direction, and the East–West component in the transversal direction. When the 100% scaled version was applied, and after 6.2 s, the structure collapsed, as shown in Figure 4.

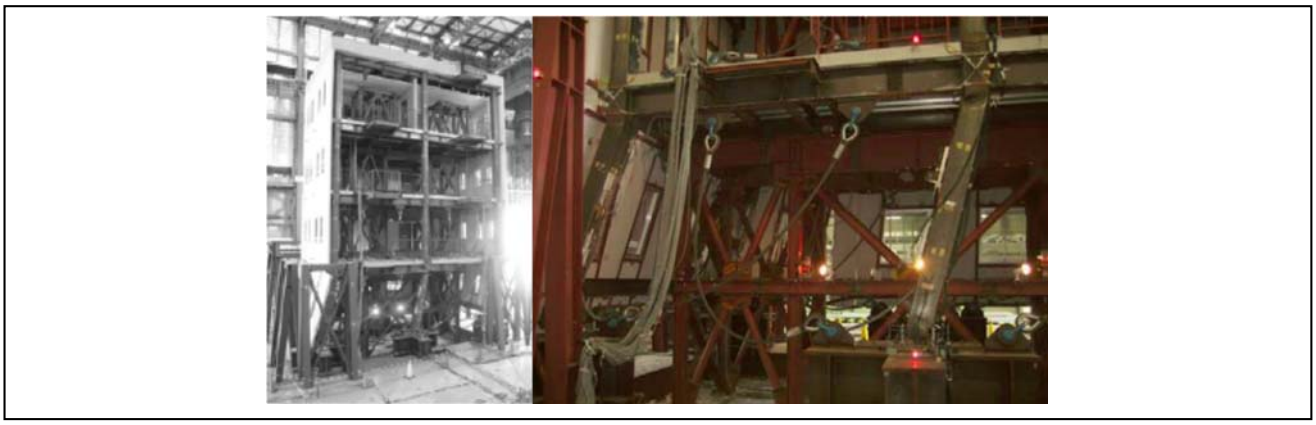

Figure 4. Structure collapsed after the 100% Takatori record

It is possible obtain more details of the prototype in [9–12].

B. Numerical modelling of the structure

According to the data of the prototype, the model that is shown in Figure 5, was implemented in the software SAP2000 [13].

Figure 5. Numerical simulation of the prototype in SAP2000

Frame elements were considered for beams and columns, and shell elements for the slabs.

Two nonlinear time–history analysis procedures were performed. One of them is the nonlinear modal time–history analysis that is an ex tension of the fast nonlinear analysis [14], where all nonlinearity is restricted to the link elements. The other procedure is the nonlinear direct integration analysis [14]. In this last case, it is possible to consider plastic hinges and material nonlinear properties.

The hinge property data that are defined in SAP2000 were selected, with interaction of P–M2–M3 (axial force and two bending moments). These hinges were located in the extreme of columns in each story.

Material nonlinear properties were considered for the steel of beams and columns. A bilinear constitutive law, with 5% kinematic strain hardening were selected.

A constant damping for all the modes, equal to 2% was selected.

The fundamental periods in the longitudinal T_L and torsional T_T directions were obtained with linear eigenvalue analysis. These values are T_L= 0.916 s and T_T = 0.266 s.

The response of this model was compared with measurements obtained during the test, for the prototype subject to the 60% scaled Takatori record. Like this, the maximum values of the relative displacement, the maximum values of the drift angle, and the maximum values of the absolute acceleration are compared in Figure 6. In this Figure, only the responses in the longitudinal direction were considered, because in this direction the retrofitted was installed.

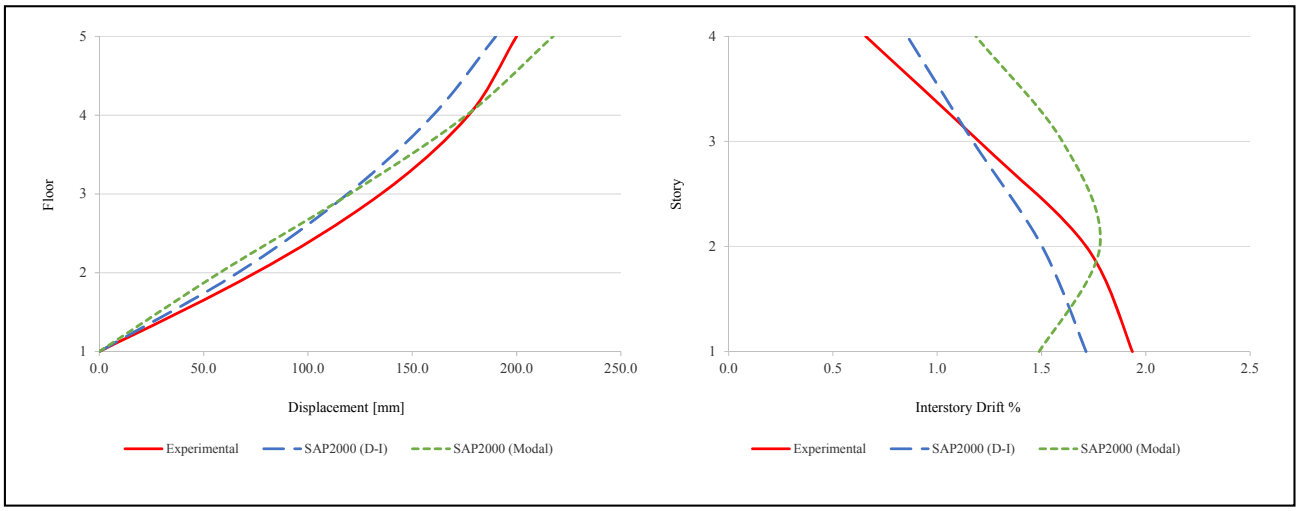

a) Maximum values of the relative displacement

b) Maximum values of the drift angle

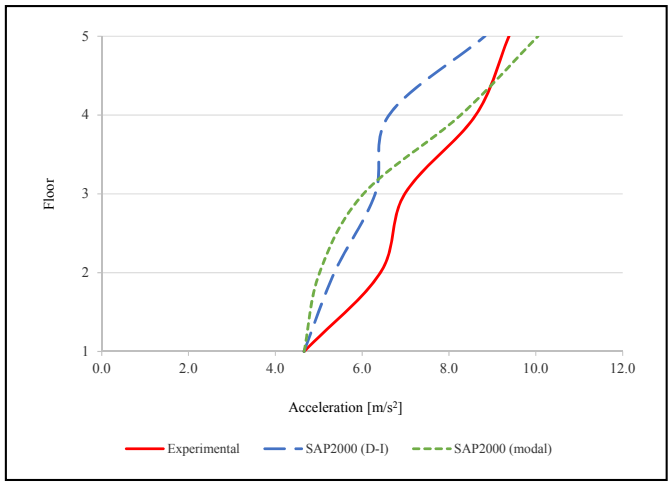

c) Maximum values of the absolute acceleration

Figure 6. Numerical vs. experimental values

According to the plots in Figure 6, it is considered that the accuracy of the model is adequate.

III. CONSIDERED ENERGY DISSIPATORS

The structure was retrofitted only in the longitudinal direction. Then energy dissipators were installed in this direction, in the diagonal of the each bay, as shown in Figure 7.

In this section, the procedures to design the BRB and the viscous dampers are presented; the constitutive models of these dissipators are also described.

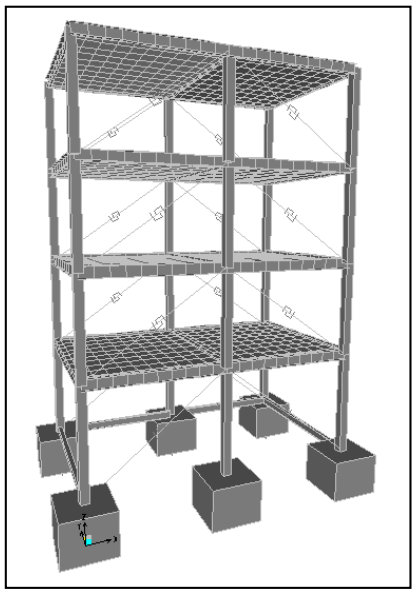

Figure 7. Numerical model of the prototype retrofitted with energy dissipators in the longitudinal direction

A. Buckling–restrained braces

Two different methods were used to design the BRB, one proposed by Palazzo [5], and the other proposed by Filiatrault and Cherry [15].

The steps of design in the Palazzo's method are:

- The analysis of the structure without dissipators is carried out. Thus, the inter–story drifts are determined.
- First design of the BRB: The geometry of the dissipators is proposed (position, length, and angle respect to the horizontal); and the mechanical properties of the steel used in the core bar is defined. The length of the plastic zone and the stiffness of the BRB have to be defined. The stiffness is established according to the first modal shape (modal vector) and to the determined inter–story drifts. Then, it is possible to obtain the area of the transversal section of the BRB's core bar. And finally, the yield strength for each dissipators is calculated.
- The analysis of the structure with dissipators is carried out. The structure and the dissipators are verified.

In the numerical simulation, the BRB are modeled with the Bouc–Wen macro model. Black et al. [6] present studies on the effectiveness of this model to simulate the behavior of the selected dissipator. The obtained parameters for the BRBs (with Palazzo's methodology) are shown in Table IV.

TABLE IV. BRB`S PARAMETERS IN PALAZZO'S PROCEDURE

Story	Stiffness [kN/m]	Yield strength [kN]	Post yield stiffness ratio	Yielding exponent
4	3153.31	18.84	0.1	2.0
3	12613.26	75.36	0.1	2.0
2	28379.83	169.56	0.1	2.0
1	28379.83	169.56	0.1	2.0

The Filiatrault and Cherry`s method is based in the optimum hysteretic damping design spectrum [16]. This spectrum establishes the relationship between V_0/W and T_g/T_u, by function Q. V_0 is the total shear force required to activate all the hysteretic dampers in the structure, W is the seismic weight, T_g is the predominant period of the ground motion, and T_u is the fundamental period of the unbraced structure. The Q function depends on the number of floors of the buildings, the predominant period of ground motion, the fundamental period of the unbraced structure, and the fundamental period of the braced structure T_b.

In this procedure, if W, T_g, T_u and T_b are known, Q and V_0 are calculated. Then, the total activation shear is uniformly distributed among the bracing at each story, obtaining in this manner the optimum activation load for each dampers.

The obtained parameters for the BRBs (with Filiatrault's methodology) are shown in Table V.

TABLE V. BRBS PARAMETERS IN FILIATRAULT AND CHERRY'S PROCEDURE

Story	Stiffness [kN/m]	Yield strength [kN]	Post yield stiffness ratio	Yielding exponent
1 to 4	7094.96	42.39	0.1	2.0

In the E–Defense frame the design values are $T_g = 0.2$ s, $T_u = 0.9164$ s and $T_b = 0.50$ s. Then $Q = 0.4301$, and $V_0 = 553.65$ kN. The value of the activation force for each BRB is 42.2kN. With this value, and considering a yield stress of 240 MPa, a 15 mm BRB diameter was obtained for the core bar. In this design method all the steel core bars have de same diameter.

B. Viscous dampers

The design of the linear viscous damping device is based on a distribution of damping proportional to the inter–story lateral stiffness of the existing frame [16].

The steps of this method are:

- The properties of the initial unbraced structure are computed including its fundamental period T_1 (in E–Defense frame is $T_1 = 0.9164$ s).
- The desired first mode viscous damping ratio to be supplied by the viscous dampers ξ_1, must be selected (in this paper $\xi_1 = 35\%$).
- The required fundamental period of a fictitiously braced structure T_{1-f} is computed.
- A set of fictitious springs is then introduced at the proposed locations of the linear viscous dampers and are distributed according to the lateral stiffness of the unbraced structure. The stiffness constants of these springs must yield a fundamental period of the fictitious braced structure equal to T_{1-f}.
- The required viscous damping coefficient of each viscous damper C_L is computed as proportional to the stiffness constants for the fictitious springs obtained in the last step. The initial structure is then fitted with dampers with the corresponding value of C_L.
- The final bracing member sections are then selected based on the anticipated maximum force in each viscous damper.
- The final design of each linear viscous damper is performed based on the required damping constant, anticipated maximum force and stroke.

The viscous damper was modelled in SAP2000 with a "damper link" element. The viscous damping coefficients of each damper C_L are presented in Table VI.

TABLE VI. VISCOUS DAMPING COEFICIENT

Story	**C_L [kNs/m]**
4	3654
3	7886
2	7726
1	7191

IV. NUMERICAL RESULTS

In the first part of this section, the two BRB's design procedures are compared. Then, a comparison between the free structure, the structure with BRB and the structure with viscous dampers is performed.

A. Comparison between the design methodologies for BRB

In Figure 7, a comparison of the displacements and accelerations obtained between the two design methods and between the two integration algorithms is shown. It must be pointed out that for the modal integration algorithm the analysis took 45 seconds and for the direct integration algorithm the analysis took 3 hours.

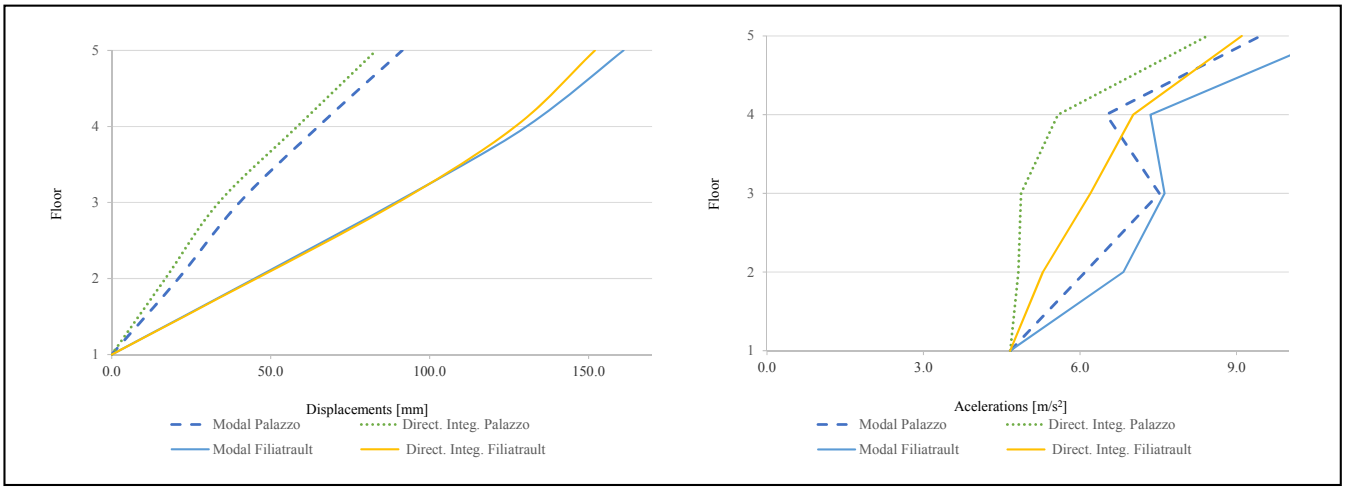

Figure 8. Maximum story displacements and story accelerations values in the structure with BRB for the two design methods and two integration algorithms

The displacements of the Palazzo's design method calculated with the direct integration algorithm vary by 16% from those of the modal integration algorithm. The displacements of the Filiatrault's design method calculated by the modal and the direct integration algorithms show a variation of 2%.

The acceleration values are more scattered; for the Palazzo's method there is a 27% average variation between the two integration algorithms. For the Filiatrault's method, the variation in the acceleration is 19% between the modal and the direct integration algorithms.

In Figure 8 the final deformed configurations of the steel frame are shown, for the Palazzo's method and for the Filiatrault's method, respectively. The steel frame retrofitted with the BRB designed with Pallazo's method remain elastic and without residual deformations; conversely, the steel frame retrofitted with the BRB designed with Filiatrault's method has undergone plastic deformations and a number of plastic hinges have been formed on the columns.

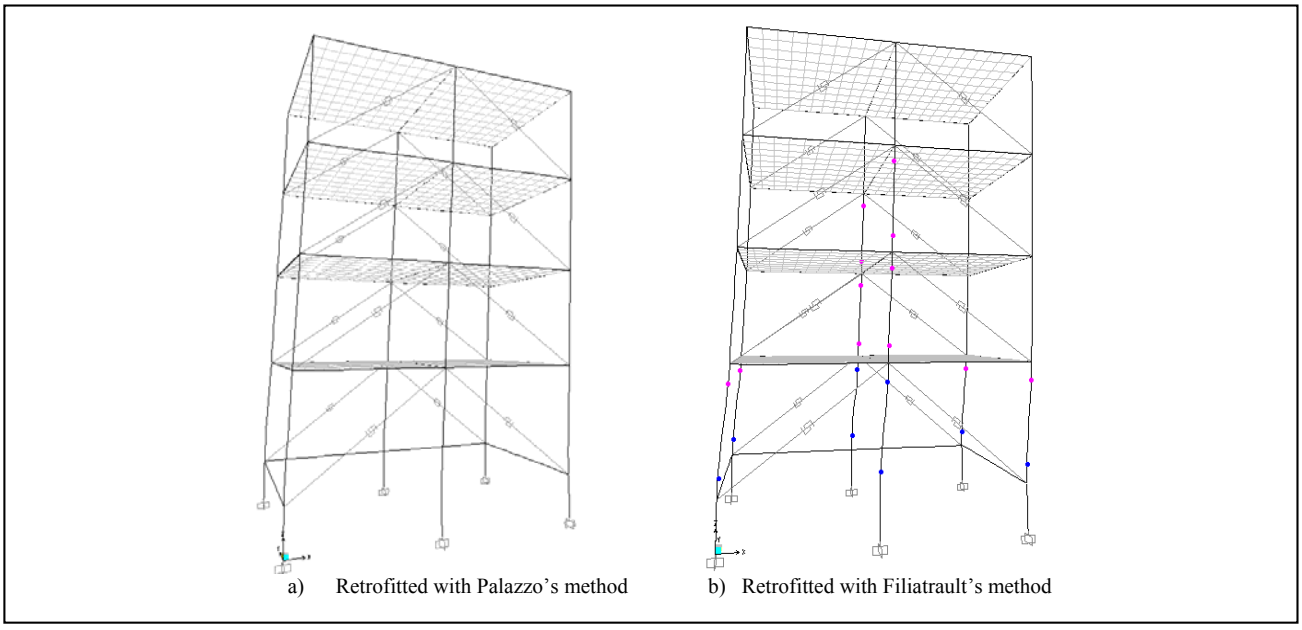

a) Retrofitted with Palazzo's method b) Retrofitted with Filiatrault's method

Figure 9. Final stages of the models

The displacements obtained through the Palazzo's design method are 55% lower than the ones obtained using the Filiatrault's method. A 15% reduction in the acceleration is also observed.

B. Comparison between the bare frame, the frame with BRBs and the frame with viscous dampers

In Figure 10 the comparison of the maximum relative displacement and absolute acceleration for each story for the structure with/without dampers, undergoing the 60% scaled Takatori record is shown. In this case, the nonlinear direct integration analysis was used. A 66% average reduction of maximum displacement in each story was achieved with the implementation of BRB. With the viscous dampers devices, the reduction in the displacements was 89%. The acceleration also exhibits a reduction in its maximum values; 16% of average reduction was achieved for the structure with BRB, and a 32% for the structure with viscous damper devices. It must be noticed that for the viscous damper devices the accelerations remain almost constant trough all stories, avoiding the effect of magnification of accelerations in height.

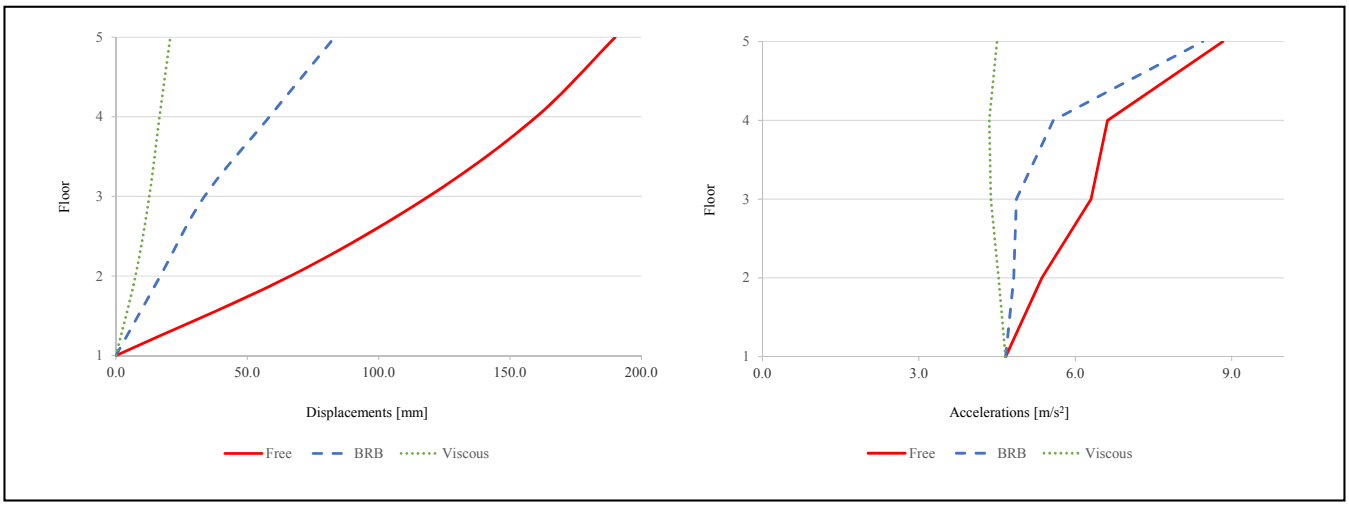

Figure 10. Maximum story displacements and story accelerations in the structure with/without dissipators (nonlinear direct integration analysis)

The values of displacements and accelerations were also calculated using the nonlinear modal time–history analysis; they are showed in Figure 11. The reductions in displacement were 62% for the structure with BRB and 89% for the structure with viscous damper devices. For the accelerations, a decrease of the 5% was achieved with the BRB and a 35% with the viscous dampers devices.

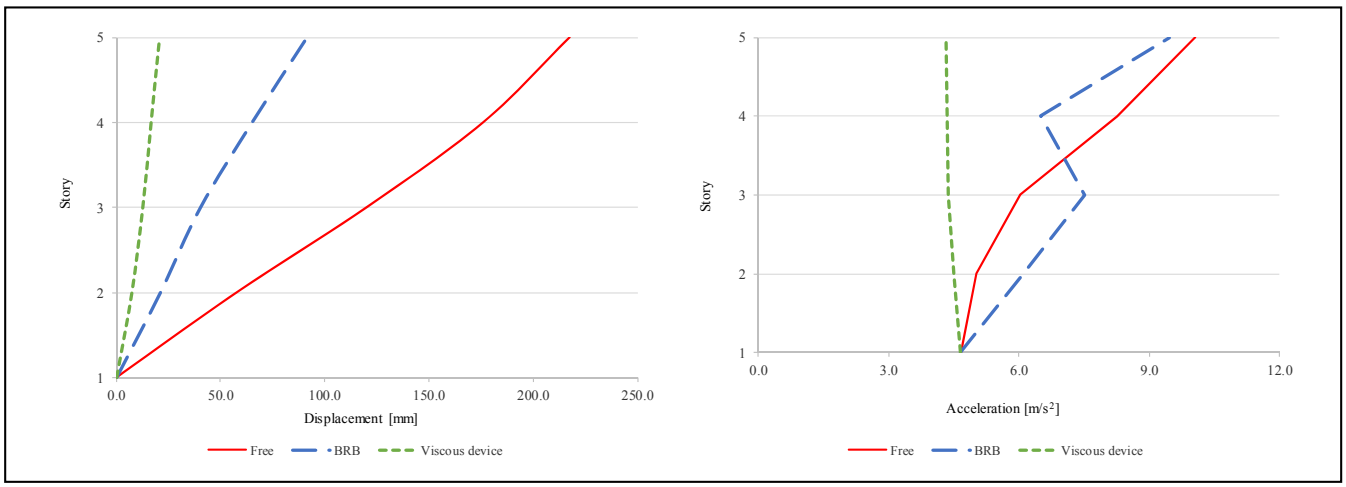

Figure 11. Maximum story displacements and story accelerations in the structure with/without dissipators (nonlinear modal time–history analysis)

In Figures 12 and 13 the time history of accelerations and displacements obtained with the nonlinear modal time–history analysis in the top floor for the structure with/without dampers are presented.

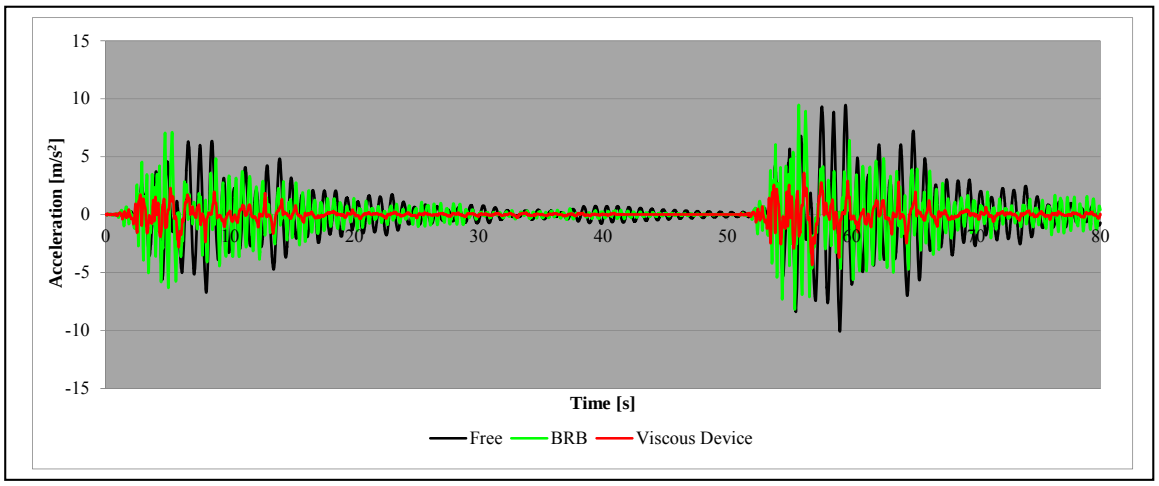

Figure 12. Time–history accelerations in the top floor (nonlinear modal time–history analysis)

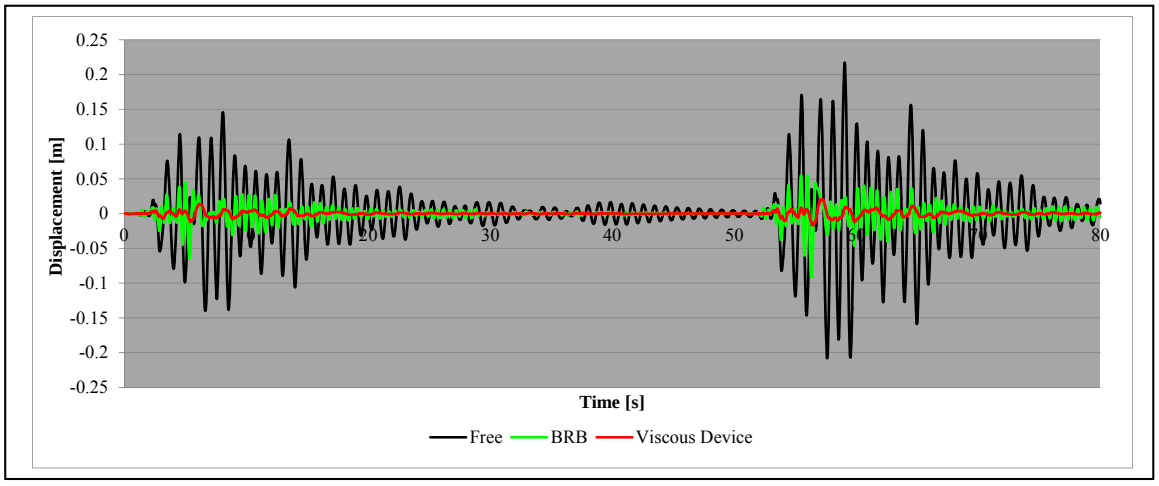

Figure 13. Time–history displacements in the top floor (nonlinear modal time–history analysis)

The time history of displacements and acceleration for the structures with/without dampers obtained using nonlinear direct integration analysis are shown in Figure 14 and 15.

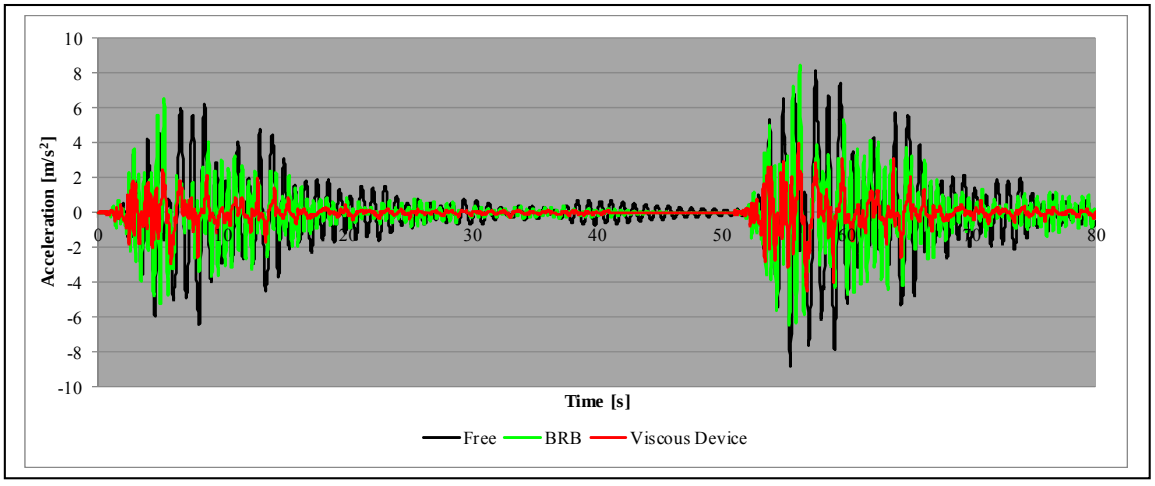

Figure 14. Time–history accelerations in the top floor (nonlinear direct integration analysis)

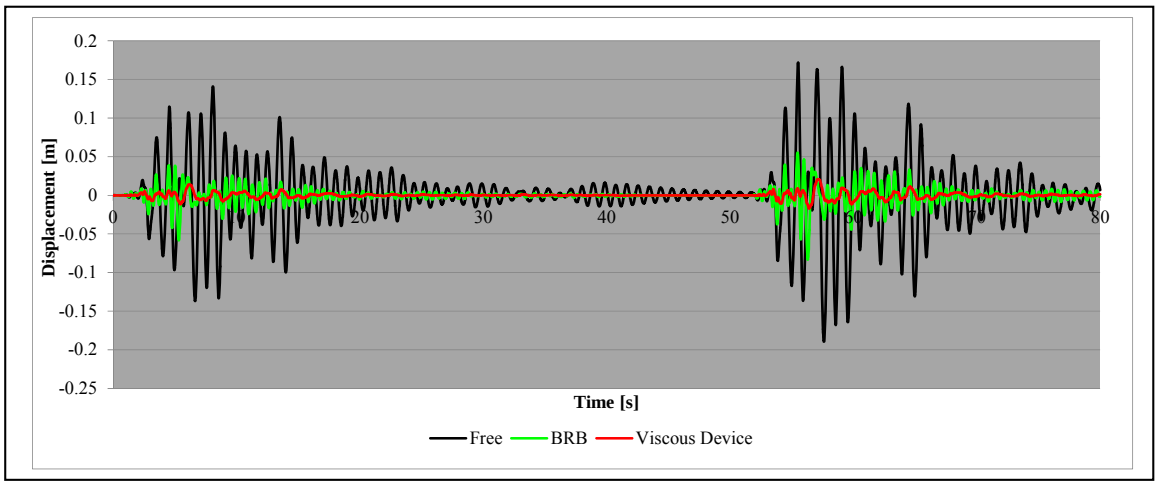

Figure 15. Time–history displacements in the top floor (nonlinear direct integration analysis)

V. CONCLUSIONS

This paper presents a numerical study of a 4–story steel moment–resisting frame that was retrofitted with two different approaches, one with the use of BRB and the other with viscous dampers devices. Two design methods were used for the BRB and one for the viscous damper devices. Then the structures were subjected to the near–fault motion recorded during the Kobe earthquake in Takatori. Two different nonlinear time–history analysis available in the finite element program SAP2000 were used. Particular conclusions are summarized below:

- For the structure retrofitted with BRB, the displacements obtained with the Palazzo's design method are considerably smaller than those obtained with the Filiatrault's design method are. Since the structure retrofitted with the Filiatrault's design method underwent plastic deformations and the displacements decreased only a 24%, this method is no longer considered.
- The nonlinear modal time–history analysis of the structure retrofitted with BRB lasted 45 seconds, which is considerably less than the 3 hours that lasted the nonlinear direct integration analysis. However, there was a difference of 16% in the values of the displacements and 27% in the values of the accelerations between the results of the two nonlinear time–history analyses.
- 52 hours were necessary to complete the nonlinear direct integration analysis of the structure with viscous damper devices, and 58 seconds demanded to complete the analysis with the nonlinear modal time–history analysis. The difference obtained in the values of accelerations and displacements between the two nonlinear time–history analyses was less than 1%.
- The BRBs designed with Palazzo's method, lead to a reduction of 66% in displacements compared with the structure without dampers. As regards to the viscous dampers, the reduction of displacements was of 89%.
- The reduction in the acceleration was not as remarkable as the reduction in the displacements for the structure with BRB, the reduction achieved was 13%. For the structure with viscous dampers, the reduction was 32%, but must be remarked that with these devices the accelerations were approximately equal in each story avoiding the magnification of accelerations in height.
- In terms of acceleration and displacement, the viscous dampers are a more effective way to retrofit the considered structure.

ACKNOWLEDGMENT

The authors thanks the support of the National Agency of Science and Technology of Argentina and the collaboration of the civil engineering student Alejandro Forte.

REFERENCES

[1] Housner G.W., Bergman L.A., Caughey T.K., Chassiakos A.G., Claus R.O., Masri S.F., Skelton R.E., Soong T.T., Spencer B.F., Yao J.T.P. (1997). Structural Control: Past, Present, and Future. Journal of Engineering Mechanics ASCE; 123:897−971.

[2] Soong T., Dargush G. (1997). Passive energy Dissipation Systems in Structural Engineering, John Wiley.

[3] Martelli A. (2006). Modern seismic protection systems for civil and industrial structures. An advanced approach to earthquake risk scenarios, with applications to different European towns. Downloadable at http://www.samco.org/network/download_area/paper_martelli.pdf.

[4] Watanabe A., Hitomi Y., Saeki E., Wada A., Fujimoto M. (1988). Properties of Brace Encased in Buckling–Restraining Concrete and Steel Tube. Proceedings of the Ninth World Conference on Earthquake Engineering. Vol. IV. 719–724. Japan Association for Earthquake Disaster Prevention. Tokyo–Kyoto. Japan.
[5] Palazzo G. (2009). Rehabilitation of seismic RC frames through buckling restrained braces. PhD Dissertation (in Spanish), National Technological University, Mendoza, Argentina.
[6] Black C., Makris N., Aiken L. (2004). Component testing, seismic evaluation and characterization of buckling restrained braces, Journal of Structural Engineering ASCE 130:329–337.
[7] Palazzo G., López-Almansa F., Cahís X., Crisafulli F. (2009). A low-tech dissipative buckling restrained brace. Design, analysis, production and testing. Engineering Structures. 31(9):2152-2161.
[8] Clark P., Aiken I., Kasai K., Ko E., Kimura I. (1999). Design Procedures for Buildings Incorporating Hysteretic Damping Devices. Proceedings of the 68th Annual Convention. Structural Engineers Association of California. Sacramento; 355–371.
[9] Tada M., Ohsaki M., Yamada S., Motoyui S., Kasai K. (2007). E–Defense Test on Full–Scale Steel Buildings: Part 3– Analytical Simulation of Collapse, NEES/E–Defense collaborative research program on steel structures.
[10] Yamada S., Suita K., Tada K., Kasai K., Matsuoka Y., Shimada Y. (2008). Collapse experiment on 4–story steel moment frame: Part 1 outline of test results. 14th World Conference on Earthquake Engineering, Beijing, China.
[11] Ohsaki M., Kasai K., Thiagarajan G., Yang Y., Komiya Y. (2008). 3–D analysis methods for 2007 blind analysis contest. 14th World Conference on Earthquake Engineering, Beijing, China.
[12] Pavan A. (2008). Blind prediction of a full–scale 3D steel frame tested under dynamic conditions. MSc Dissertation, Centre for Post–Graduate Training and Research in Earthquake Engineering and Engineering Seismology (ROSE School), Pavia, Italy.
[13] SAP 2000 (2000). Computers and Structures Inc.
[14] Wilson E.L. (1985). A New Method of Dynamic Analysis for Linear and Nonlinear System, in Finite Element in Analysis Design, 1:21–23.
[15] Filiatrault A., Cherry S. (1990). Seismic design spectra for friction damped structures, ASCE journal of Structural Engineering, 116(5):1334–1355.
[16] Christopoulos C., Filiatrault A. (2006). Principles of Passive Supplemental Damping and Seismic Isolation, IUSS PRESS, Pavia, Italy.